

Behaviour of flush end-plate beam-to-column joints under bending and axial force

Luís Simões da Silva†

Civil Engineering Department, University of Coimbra, Polo II, Pinhal de Marrocos, 3030 Coimbra, Portugal

Luciano R. O. de Lima‡ and Pedro C. G. da S. Vellasco‡†

Structural Engineering Department, UERJ - State University of Rio de Janeiro, Brazil

Sebastião A. L. de Andrade‡†

Civil Engineering Department, PUC-RIO - Pontifical Catholic University of Rio de Janeiro, Brazil

(Received August 12, 2002, Accepted January 26, 2004)

Abstract. Steel beam-to-column joints are often subjected to a combination of bending and axial forces. The level of axial forces in the joint may be significant, typical of pitched-roof portal frames, sway frames or frames with incomplete floors. Current specifications for steel joints do not take into account the presence of axial forces (tension and/or compression) in the joints. A single empirical limitation of 10% of the beam's plastic axial capacity is the only enforced provision in Annex J of Eurocode 3. The objective of the present paper is to describe some experimental and numerical work carried out at the University of Coimbra to try to extend the philosophy of the component method to deal with the combined action bending moment and axial force.

Key words: component method; experimental analysis; flush end-plate joints; semi-rigid behaviour; bending and axial force.

1. Introduction

Beam-to-column joints are often subjected to a combination of bending and axial forces. Although in many regular building frames the level of axial force coming from the beam is usually low, it can reach significant values in many instances, such as:

- (i) Regular frames under significant horizontal loading (seismic or extreme wind), especially for sway frames;
- (ii) Irregular frames under gravity or horizontal loading, especially with incomplete floors;
- (iii) Pitched-roof portal frames.

†Professor

‡Ph. D.

‡†Associate Professor

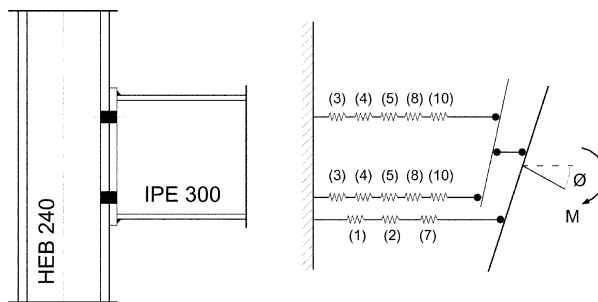


Fig. 1 Component model for flush end-plate beam-to-column joint in bending

The component method, (Faella *et al.* 2000), as stated in Annex J of Eurocode 3 (1998), or, with an improved and enlarged scope, in Part 1.8 of Eurocode 3 (2003), consists of a simplified mechanical model composed of extensional springs and rigid links, whereby the connection is simulated by an appropriate choice of rigid and flexible components. These components represent a specific part of a connection that, dependent on the type of loading, make an identified contribution to one or more of its structural properties. A typical component model for a flush end-plate beam-to-column joint is illustrated in Fig. 1, the relevant components being (1) column web panel in shear, (2) column web in compression, (3) column web in tension, (4) column flange in bending, (5) end-plate in bending, (7) beam flange and web in compression, (8) beam web in tension and (10) bolts in tension. In general, each of these components is characterised by a non-linear force-displacement curve, although simpler idealisations are possible, whenever only the resistance or the initial stiffness of the connection is required. Application of the component method to steel joints requires the following steps:

- (i) Selection of the relevant (active) components from a global list of components (20 different components currently codified, for example, in Part 1.8 of Eurocode 3);
- (ii) Evaluation of the force-deformation response of each component;
- (iii) Assembly of the active components for the evaluation of the moment-rotation response of the joint, using a representative mechanical model.

Currently, no specific procedures are available for the analysis and design of beam-to-column joints under bending and axial force. A single empirical limitation to an applied axial force of 10% of the beam plastic resistance under axial force is the only enforced provision of Annex J, below which the axial force may be disregarded in the analysis/design of the joint. However, the general principles of the component method cover this situation, since any component is fully characterised independently from the type of loading applied to the joint; in fact, as already stated above, the behaviour of any component is established as a force *vs.* displacement curve that only depends on the level of axial force.

Recently, some preliminary attempts were addressed at the prediction of the behaviour of beam-to-column joints under bending and axial force. In Liège, Jaspart *et al.* (1999), and Cerfontaine (2000), have applied the principles of the component method to establish design predictions of the M-N interaction curves and initial stiffness. Based on the same general principles, Silva and Coelho (2000) have proposed analytical expressions for the full non-linear response of a beam-to-column joint under combined bending and axial force. Unfortunately, both results were not calibrated/validated by experimental evidence. To provide a sound basis for further theoretical developments, an experimental program was carried out at the University of Coimbra on flush and extended end-plate beam-to-column configurations, that is described in the next section.

Next, component models able to deal with bending and axial force are presented and applied to simulate

the behaviour of the tested joints. These comparisons show clearly that, using an adequate strategy to deal with the load history arising from the simultaneous application of a bending moment and an axial force, the component method is directly applicable to the analysis of these joints. In addition, the individual component characterisation also remains unchanged from earlier work on joints in bending.

2. Experimental program

2.1. Introduction

A description of an experimental testing programme in beam-to-column joints, currently being performed at the Civil Engineering Department of the University of Coimbra is presented in this section. The test programme includes 16 prototypes, 9 flush end-plate joints and 7 extended end-plate joints, described in Fig. 2(a) and (b). Here, only the flush end-plate tests will be discussed in detail. For this joint configuration, application of the Eurocode 3 procedures for bending moment alone leads to the results of Table 1 (using actual material properties and dimensions and no partial safety coefficients).

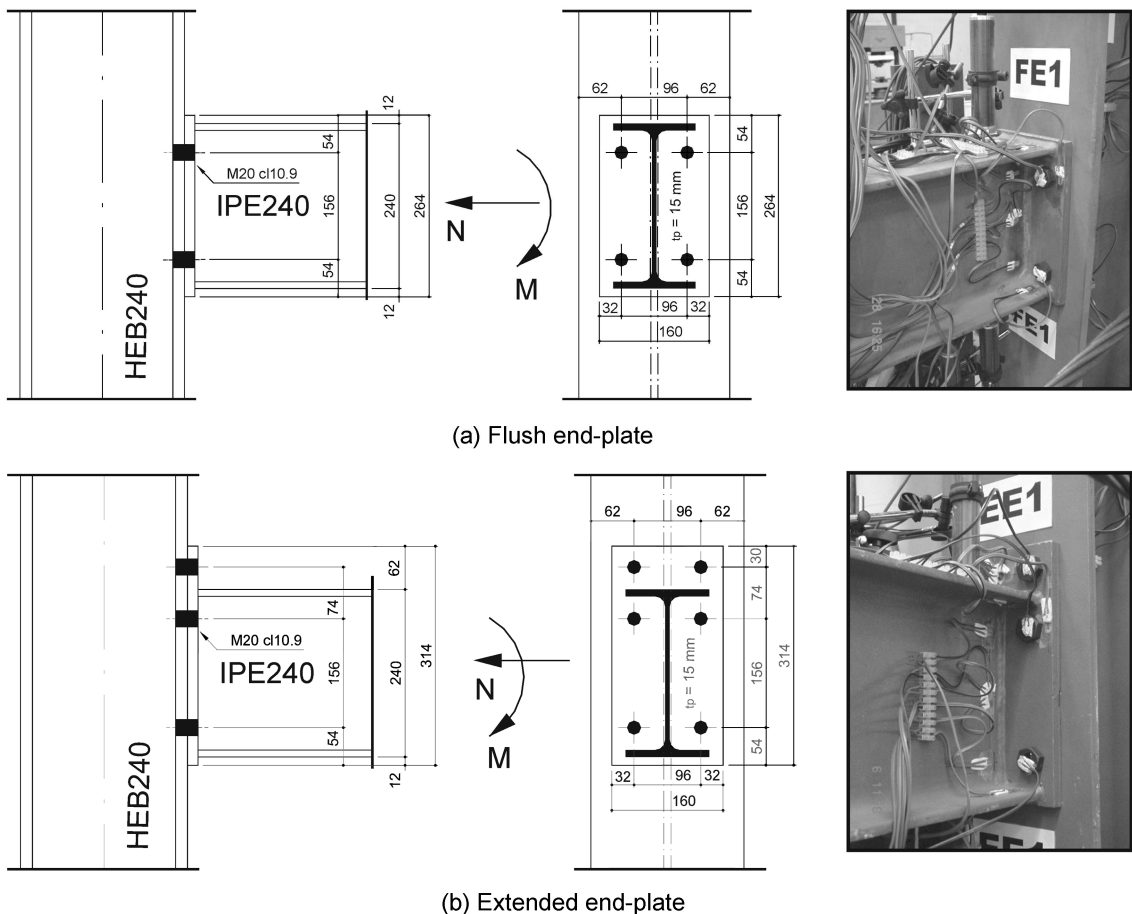


Fig. 2 Layout of joints

Table 1 Moment resistance and initial stiffness of the joints

Joint	$M_{j,Rd}$ (kN.m)	$S_{j,ini}$ (kN.m/rad)
Flush end-plate	70.0	11865.8

In all tests, the columns were simply-supported at both ends and consist of a HEB240, the beams consist of an IPE240 and the end-plate is 15 mm thick, all manufactured from steel grade S275. The bolts are M20, class 10.9.

Nine experimental tests were carried out for the flush end-plate configuration, comprising several combinations of bending and axial forces and consisting of the application of a fixed level of axial tension or compression and the subsequent application of a negative bending moment, incremented up to failure of the joint.

In the first test, FE1, only bending moment was applied through a hydraulic actuator, located a meter away from the face of the column flange. For the following tests - FE3, FE4, FE5, FE6, FE7, FE8 and FE9 - constant axial forces of, respectively, -4%, -8%, -20%, -27%, -20%, +10% and +20% of the beam plastic resistance were applied to the beam.

2.2. Test setup, instrumentation and testing procedure

The test setup is illustrated in Fig. 3 and Fig. 4(a), the bending moment being applied using a hydraulic actuator on the cantilever.

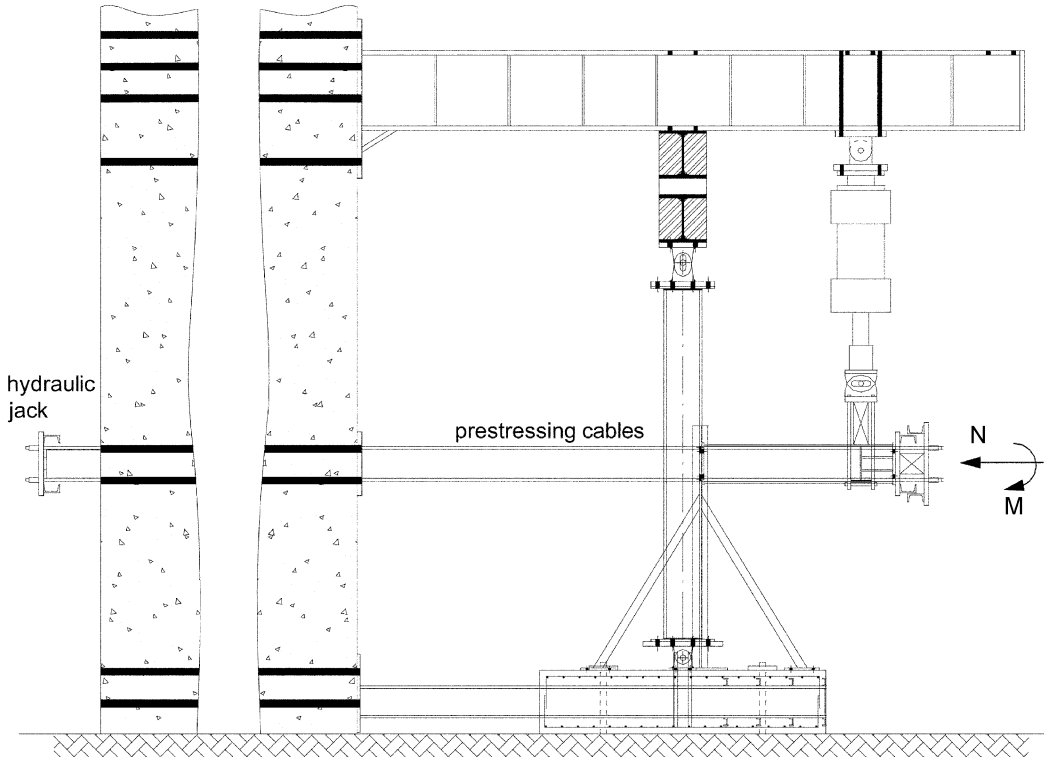


Fig. 3 Experimental test setup

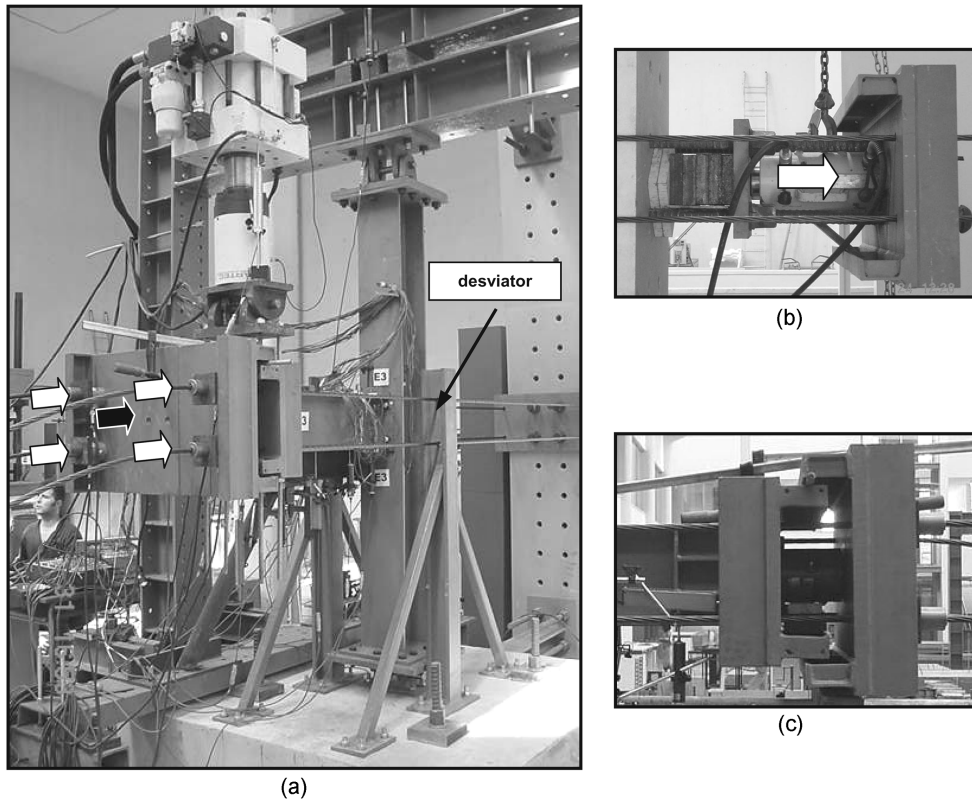


Fig. 4 (a) Loading frame for application of compressive loading, (b) hydraulic jack and (c) central load cell

The chosen system for the application of the compressive axial force consists of a hydraulic jack, Fig. 4(b), that applies a tensile force to four prestressing cables of diameter $\phi = 15.2$ mm, anchored against a reaction wall. The transfer of this force to the connection was performed through a central load cell with capacity of 950 kN (TML), Fig. 4(c). These cables pass through a deviator saddle (HEM100) to guarantee that the axial force is always parallel to the beam axis. Load cells TML with capacity of 20 0kN were installed in each cable to measure the installed force in each cable. The horizontal reaction forces at both ends of the column were transmitted to the reaction wall by (i) a steel beam, at the top, and (ii) a reinforced concrete footing prestressed to the strong floor using DYWIDAG bars and connected to the reaction wall using a HEB 200, at the bottom.

The tensile axial force application system is shown in Fig. 5. Four hydraulic jacks placed in one of the extremities of a circular hollow section profile transmit the tensile axial force. These circular profiles are simply supported at the other end to allow free rotation and to guarantee that the axial force is applied always parallel to the beam axis.

All tests were instrumented as shown in Fig. 6 and Fig. 7, with single strain gauges (FLK 6-11-TML), rosettes at 45° (FRA 5-11-TML), bolt axial strain gauges (BTM 6-C-TML), and displacements transducers (LVDT's). All data were recorded with a data acquisition system TDS602-TML.

For all tests, a constant axial force was applied first, maintained constant throughout the test, with subsequent application of a bending moment incremented to failure. Two unloading were performed,

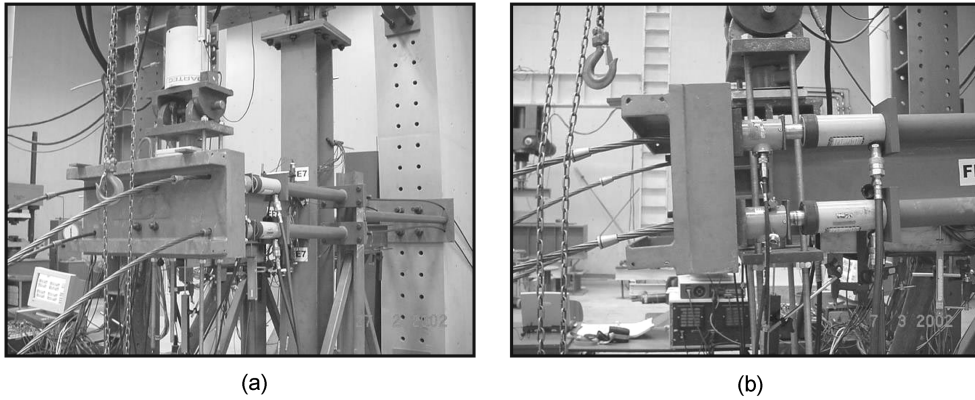


Fig. 5 (a) Application of tensile loading, (b) hydraulic jack layout

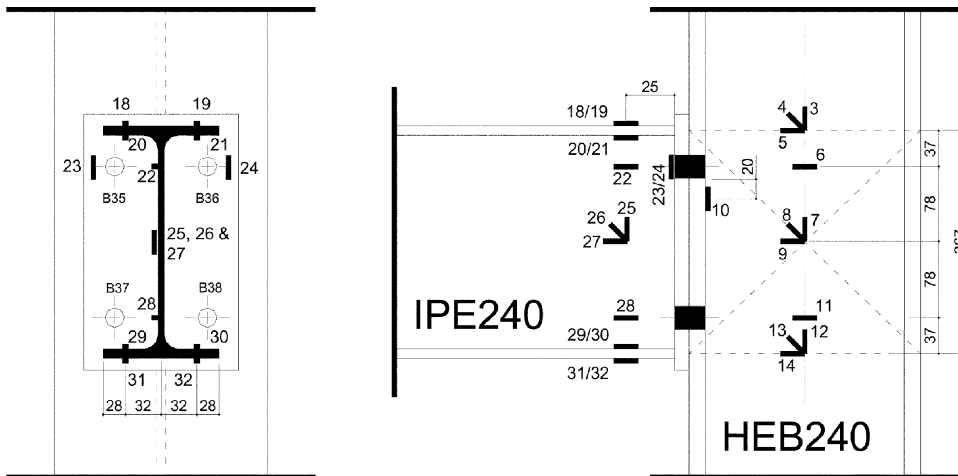


Fig. 6 Single strain gauges, rosettes to 45° and bolts axial strain gauges layout

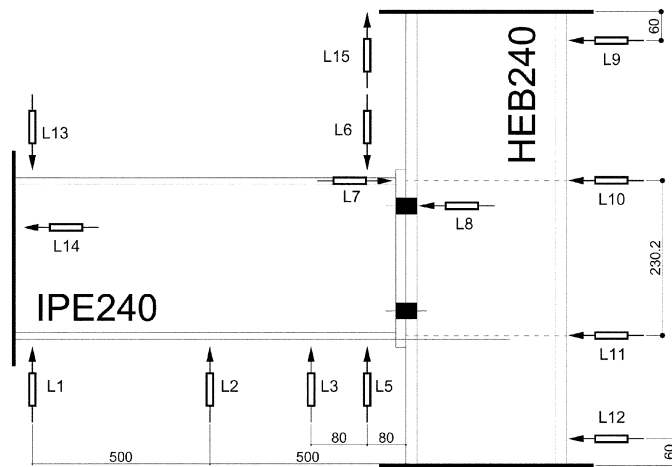


Fig. 7 Displacements transducers layout

the first for a bending moment of 25 kN.m (down to 5 kN.m, to eliminate possible slack in the joint) and the second for a rotation of 20 mrad. Force control was used in the first part of each test, subsequently changed to displacement control.

Tensile tests on coupons extracted from the beams and columns were carried out, aiming at characterizing the actual properties of the material. Then, it was possible to calculate the beam plastic resistance and to determine the true level of applied axial force to the beam for the other tests. These tensile tests were performed according to the following specifications, EN10002 (1990), EN10020 (1989) and EN10025 (1994), yielding the results of Table 2.

2.3. Application of the axial force

Given the need to ensure accurate control of the application of the axial force, an initial test was performed (FE2) in the elastic range to calibrate the application of the axial force. It was verified that the application of the axial load with the cables was transmitted by the central load cell to the connection as shown in Fig. 8. In this graph, it can be seen that the axial force applied to the connection, measured either through (i) the strain gages located in the beam web and flange, (ii) the central load cell or (iii) by superposition of the individual load cells, yields similar results.

For higher levels of bending moment, it was verified that the rotation of the beam caused a reduction of the force in the bottom cables and an increment of load of the top cables. Consequently, hydraulic jacks were placed in the bottom cables to correct the axial force as the test progressed. In Fig. 9, the variation of the axial force in each individual cable with applied moment is shown for all tests. In this figure, the clear difference between tests FE3, FE4 and FE5, and FE6, FE7, FE8 and FE9 reflects the fact that only for the latter individual hydraulic jacks were used to correct the load unbalance caused by deformation of the beam, thus leading to a virtually constant applied axial force.

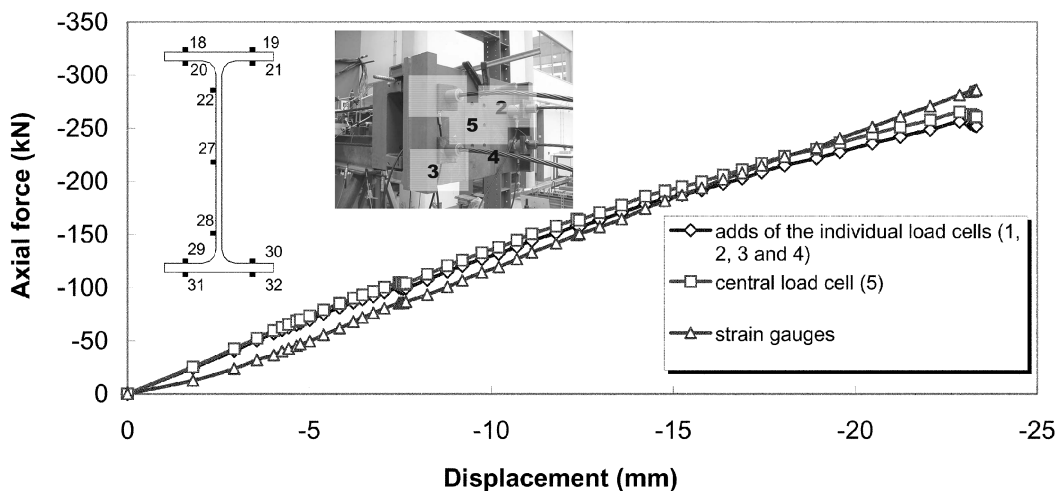


Fig. 8 Verification of applied axial force

Table 2 Steel mechanical properties

BEAM IPE240			
Specimen	f_y (MPa)	f_u (MPa)	Young's modulus (MPa)
Web_1	366.45	460.36	201483
Web_2	358.93	454.70	202836
Web_3	371.86	449.32	211839
Web_4	380.25	455.99	201544
Web_5	375.79	459.49	211308
Web_6	379.12	461.98	210128
Web_7	342.72	453.40	190443
Web_8	332.32	438.76	200127
Web average	363.4	454.3	203713
Standard deviaton	17.64	7.49	7214
Flange_1	365.83	444.52	215739
Flange_2	331.62	448.30	213809
Flange_3	340.75	448.77	212497
Flange_4	346.42	450.50	216924
Flange_5	355.40	458.90	221813
Flange_6	349.22	455.88	213589
Flange_7	312.13	443.81	214147
Flange_8	319.73	435.20	213257
Flange average	340.14	448.23	215222
Standard deviaton	18.08	7.38	3017
COLUMN HEB240			
Specimen	f_y (MPa)	f_u (MPa)	Young's modulus (MPa)
Web_1	392.63	491.82	205667
Web_2	399.38	495.29	204567
Web_7	340.16	454.39	218456
Web_8	355.92	467.69	199055
Web average	372.02	477.29	206936
Standard deviaton	28.56	19.59	8206
Flange_1	344.92	410.06	232937
Flange_2	350.09	472.93	210434
Flange_7	337.94	450.53	222665
Flange_8	338.84	461.63	217132
Flange average	342.95	448.79	220792
Standard deviaton	5.68	27.39	9516
END-PLATE			
Specimen	f_y (MPa)	f_u (MPa)	Young's modulus (MPa)
Ep1	365,39	504,45	198936
Ep2	374,75	514,44	(not available)
Ep3	380,91	497,81	199648
Ep4	356,71	497,08	202161
Web average	369,44	503,45	200248
Standard deviation	10,62	8,05	1694,36

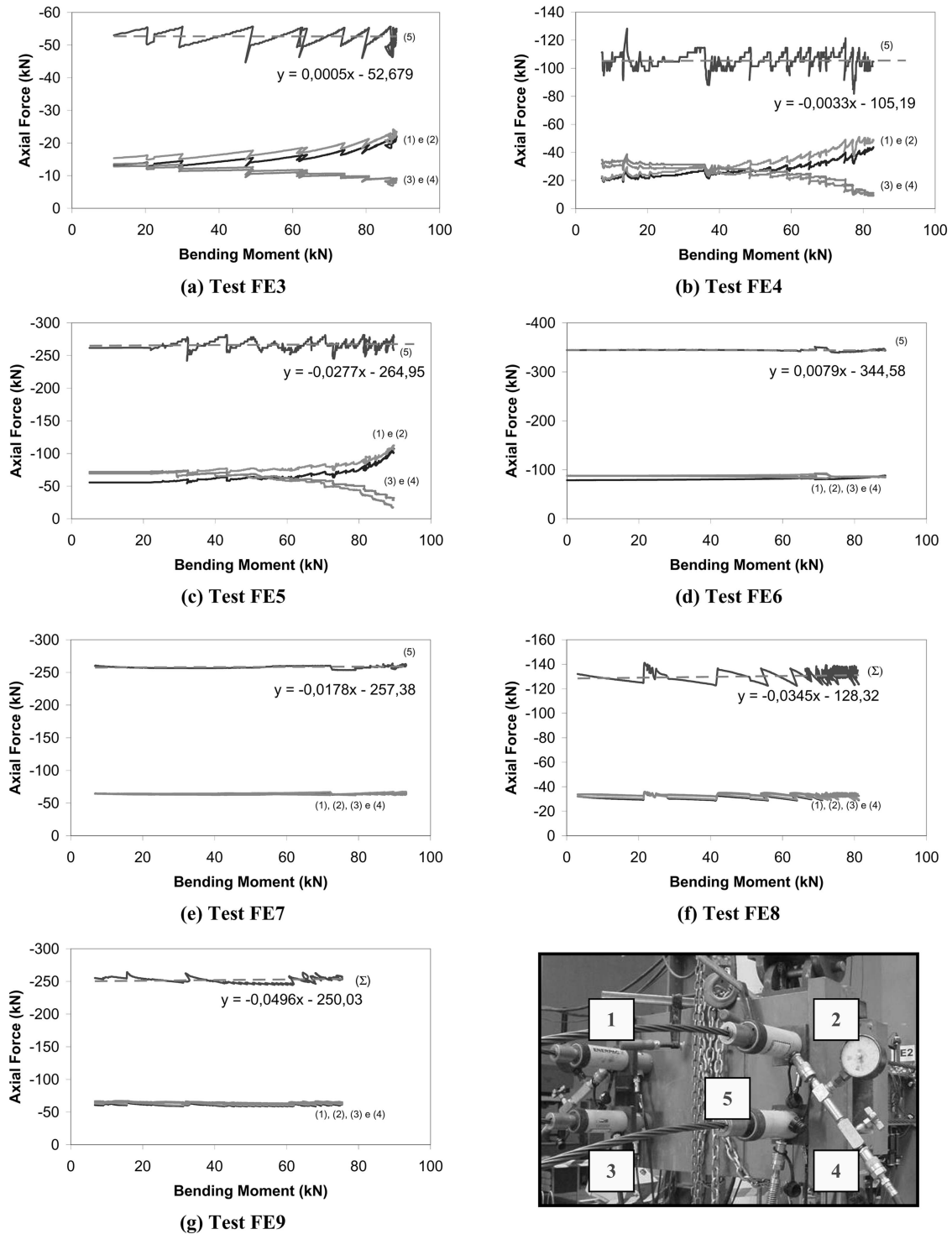


Fig. 9 Bending moment vs. axial force curves

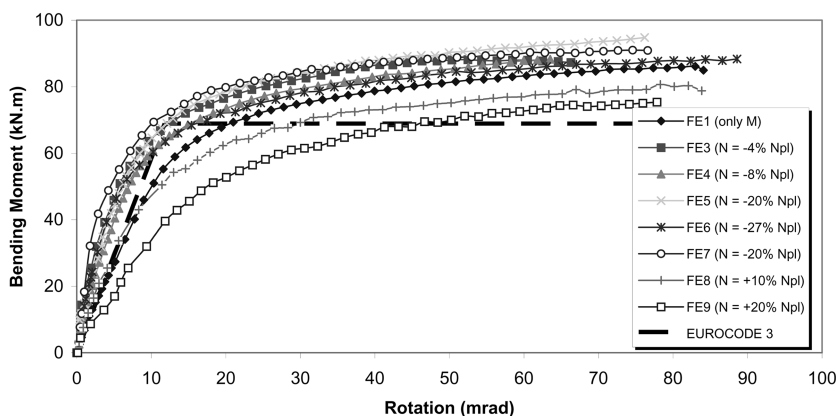


Fig. 10 Moment vs. rotation curves of the experimental tests

Table 3 Experimental values of bending moment resistance and initial stiffness

Test	N (kN)	M_{Rd} (kN.m)	$S_{j,ini}$ (kN.m/rad)
FE1 (only M)	-	68.4	7244
FE3 (-4% Npl)	52.7	76.7	9768
FE4 (-8% Npl)	105.6	73.5	10853
FE5 (-20% Npl)	265.0	78.5	10610
FE6 (-27% Npl)	345.0	72.4	9927
FE7 (-20% Npl)	265.0	80.0	8028
FE8 (+10% Npl)	130.6	62.8	8959
FE9 (+20% Npl)	264.9	52.3	9084

3. Analysis of the experimental results

3.1. Moment vs. rotation curves

The experimental moment vs. rotation curves for the eight tests are presented in Fig. 10, where it may be observed that even for a level of equivalent axial force of 27% of the beam plastic resistance, the bending moment still exceeds the pure bending result (FE1). Also, the maximum bending moment was obtained for an axial load level of 20% of the beam plastic resistance. In contrast, the application of a tensile force in the beam results in a sharp reduction of the bending resistance of the joint. Table 3 presents the values obtained for the moment resistance and the initial stiffness of the tested joints. The theoretical values calculated according to Eurocode 3 (FE1) were, respectively, 70 kN.m and 11865 kN.m/rad.

3.2. Analysis of individual components

Table 4 presents the theoretical values of the strength and initial stiffness for all components of the connection in study, calculated in accordance with Eurocode 3.

Fig. 11 shows that, for all the tests, the column flange in bending presented deformations according to mode 1, that is, complete yielding of the flange. The measured displacements for this component are presented in Fig. 12 where it is noticed that the behaviour of the component is similar for all the tests, independently of the applied axial force.

Table 4 Theoretical values of the resistance and initial stiffness of the components

Component		F_{Rd} (kN)	k/E (mm)
Tension	Column web in tension (3)	498.9	7,03
	Column flange in bending (4)	406.1	38,22
	End-plate in bending (5)	321,7	13,35
	Beam web in tension (8)	476.8	∞
	Bolts in tension (10)	441,0	7,76
Compression	Column web in compression (2)	598,2	10,40
	Beam flange in compression (7)	529.8	∞
Shear	Column web in shear (1)	601.1	7,52

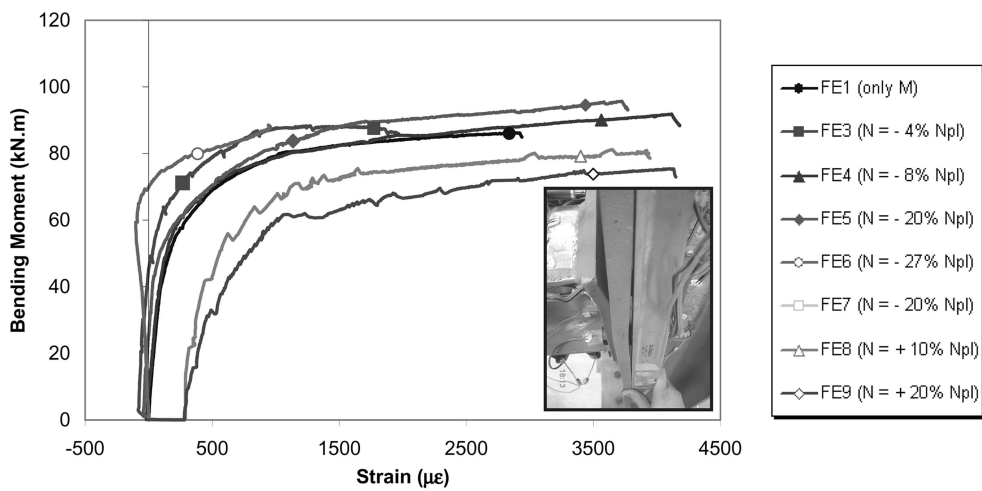


Fig. 11 Moment vs. strain curves for component column flange in bending

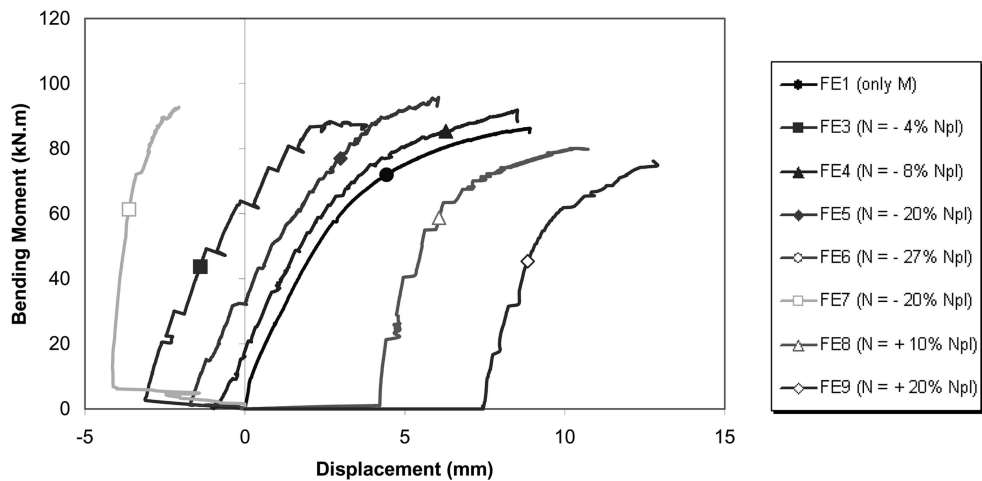


Fig. 12 Moment vs. displacements curves for component column flange in bending

Application of the design rules of Eurocode 3 yields a resistance of the end-plate in bending of 321.7 kN (Table 4). The influence of the level of axial force may be assessed from Fig. 13, by comparing, for example, tests FE1 and FE5. For test FE1, the yield strain is reached for a bending moment of, approximately, 45 kN.m. For this level of bending moment, the tensile load in the first bolt row, evaluated using the strain gages located in the beam flange, it is equal to 333.4 kN. However, for test FE5, due to the contribution of the applied axial force, the end-plate reached the yield strain at a higher level of applied moment. Fig. 14 illustrates the moment vs. displacements curves for this component.

Analysing the curves presented in Fig. 15 where the dashed line represents the yield strain obtained in the tensile tests, it is clearly noticed that the beam flange also reaches yielding. According to Eurocode 3, the resistance of the beam flange in compression is 529.3 kN. For that level of bending moment, the average of the measured strains in the bottom beam flange was 2300 $\mu\epsilon$, that is, equal to a force of 570.0 kN, higher than the theoretical value of 529.3 kN presented above; this is explained because of steel hardening. However, it is worthwhile to point out that for the first test, where the compression axial force was not applied to the beam, beam flange yielding occurred for a larger value of bending moment than in the other tests.

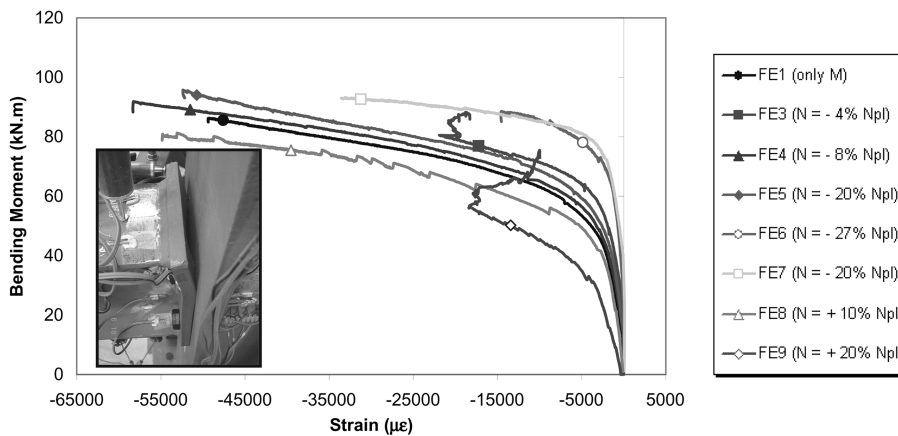


Fig. 13 Moment vs. strain curves for component end-plate in bending

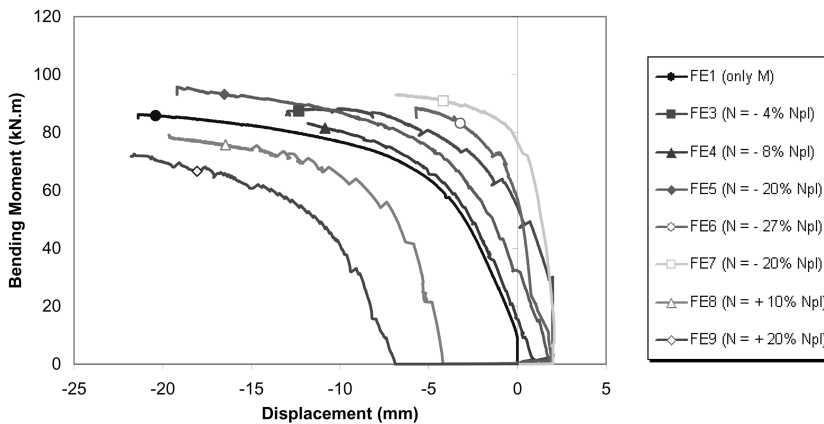


Fig. 14 Moment vs. displacements curves for component end-plate in bending

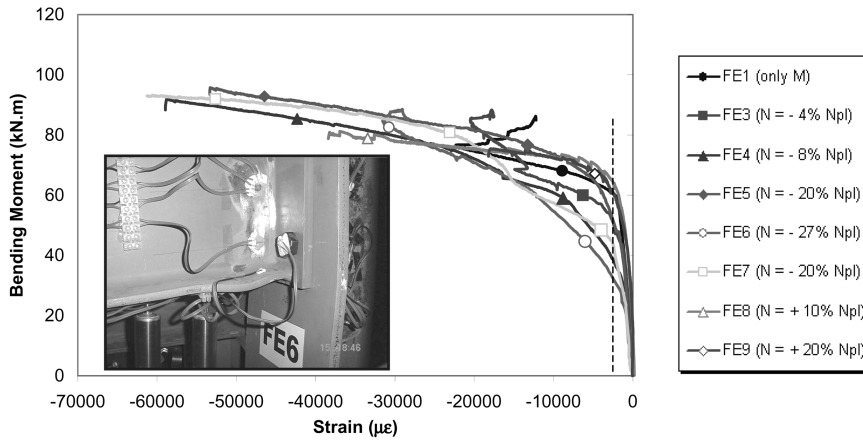


Fig. 15 Moment vs. strain curves for component beam flange in compression

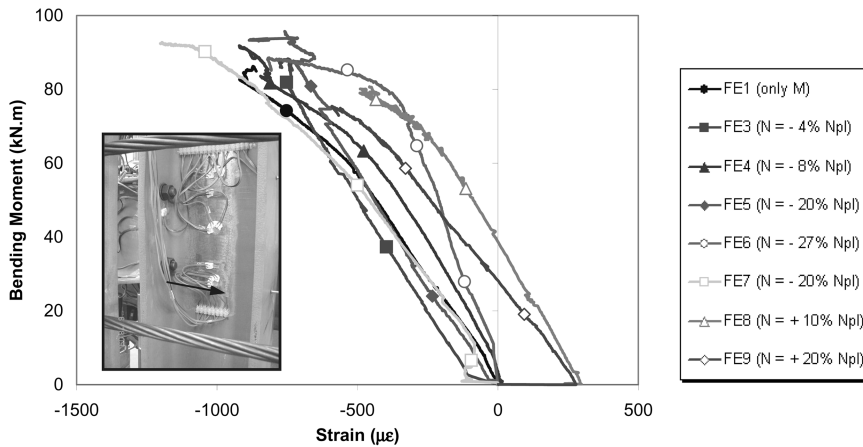


Fig. 16 Moment vs. strain curves for component column web in compression

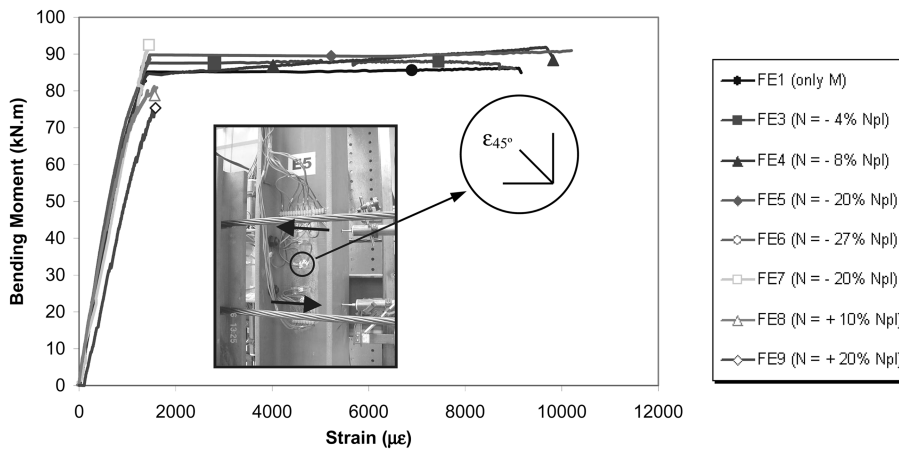


Fig. 17 Moment vs. strain curves for component column web in shear

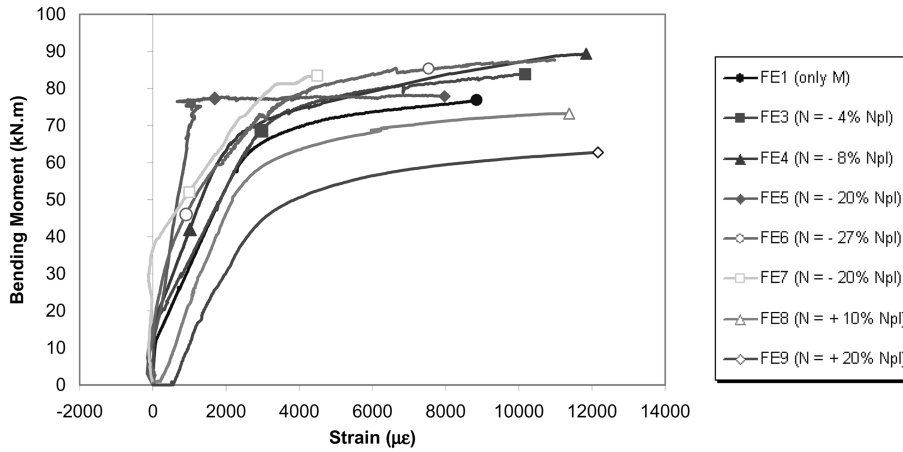


Fig. 18 Moment vs. strain curves for component bolts in tension

As can be seen in Fig. 16, except for test FE6, the component column web in compression did not reach yield for any of the tests.

The component column web in shear reached yield for tests FE1, FE3, FE4 and FE5, Fig. 17. For tests FE6 to FE9, this component did not reach yield. This graph was obtained using a rosette positioned in the centre of the column web panel.

Finally, the moment vs. strain curves for the component bolts in tension are presented in Fig. 18, where it is noticed that with the application of the compression axial force, this component is alleviated, having initially negative strains, for tests FE4, FE5 and FE6.

4. Component models for bending and axial force

Joints subjected to bending and axial force do not present distinct tension and compression zones. Following the terminology for column bases (Wald *et al.* 2000), top and bottom sides are henceforth used. These top and bottom sides must now include all possible tensile and compressive components, given that loading may vary from pure bending to pure axial force with all intermediate combinations. A resulting component model is illustrated in Fig. 19 for the same flush end-plate joint of Fig. 1. It is

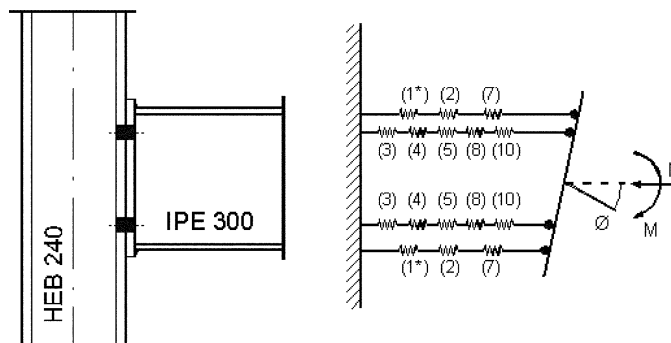


Fig. 19 Modified component model for flush end-plate beam-to-column joint

noted that the various tensile or compressive components will only become active in tension or compression, respectively, given the distinct behaviour in tension and compression, as illustrated in Fig. 20.

A final adjustment is also required to deal with the column web panel in shear that cannot be exclusively placed at the bottom side of the component model. Here, as shown in Fig. 19 (component (1*)), it is split into two equal springs characterised by the usual stiffness multiplied by a factor of 2.

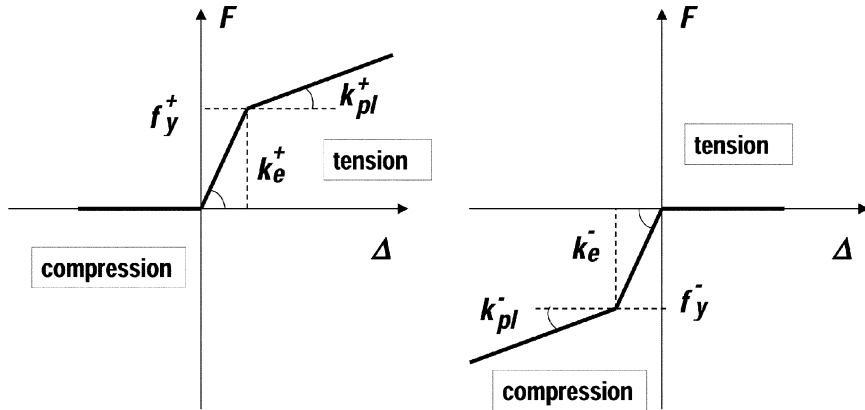


Fig. 20 Behaviour of components (springs) subjected to tension and compression

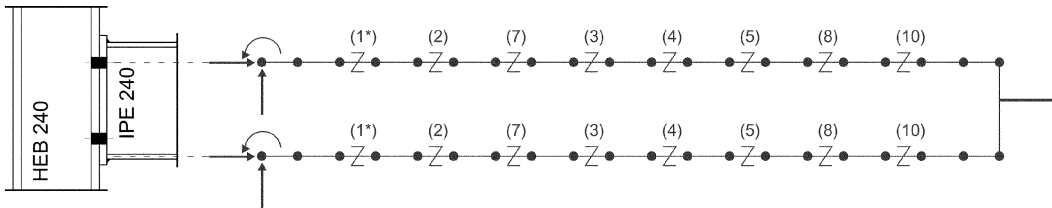


Fig. 21 Spring model for flush end-plate joints

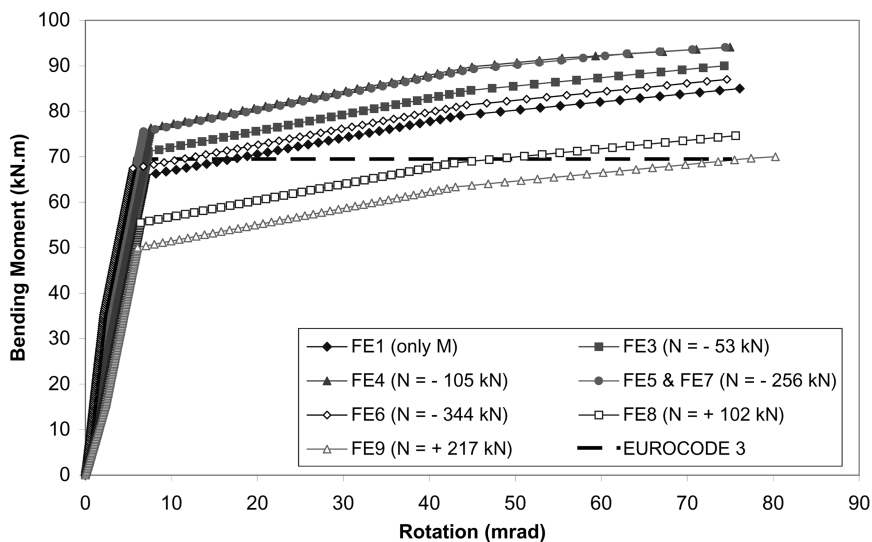
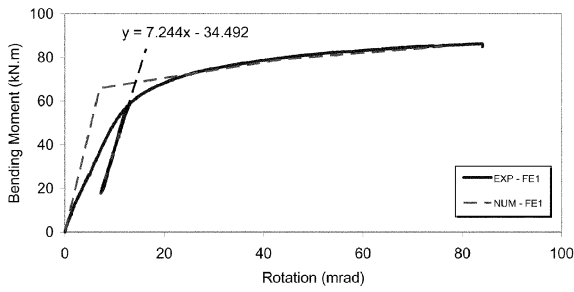
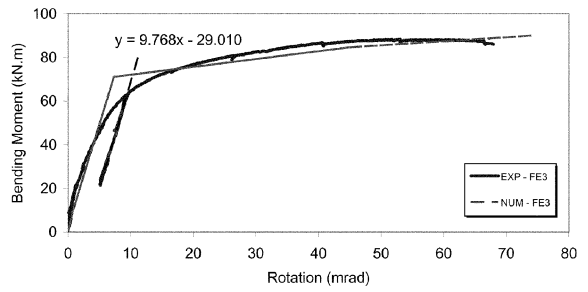


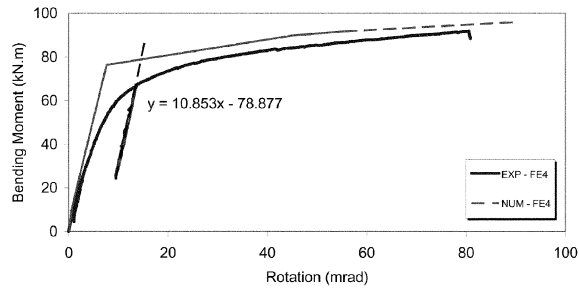
Fig. 22 Moment vs. rotation curves for tested joints obtained from numerical simulations



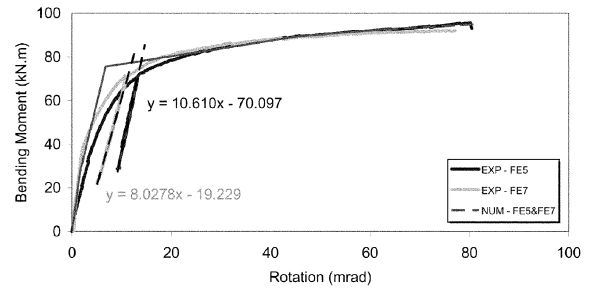
(a) FE1 (only bending moment)



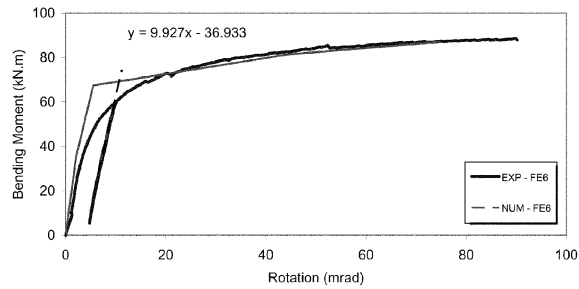
(b) FE3 (N = - 4% Npl)



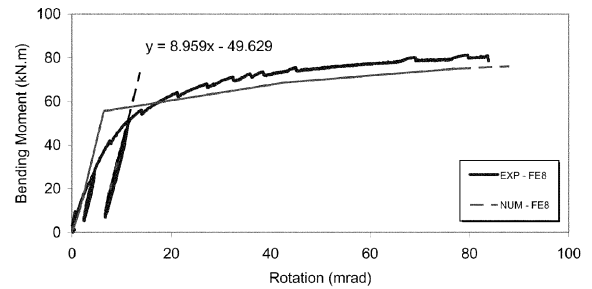
(c) FE4 (N = - 8% Npl)



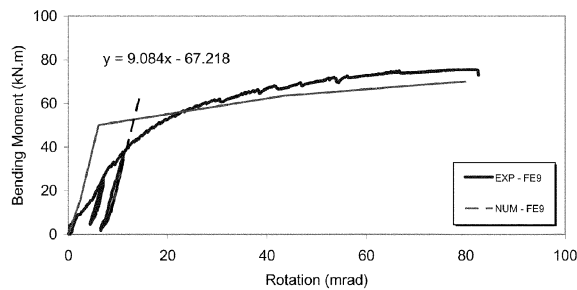
(d) FE5 and FE7 (N = - 20% Npl)



(e) FE6 (N = - 27% Npl)



(f) FE8 (N = + 10% Npl)



(g) FE9 (N = + 20% Npl)

Fig. 23 Comparison of the moment versus rotation curves

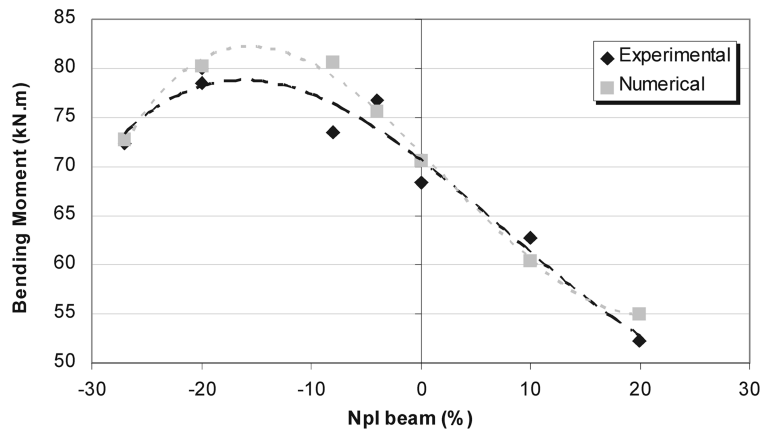


Fig. 24 M-N interaction diagram for flush end-plate joints

5. Numerical results and discussion

The flush end-plate joint of Fig. 2(a) was modelled using LUSAS Finite Element Package (2001), as shown in Fig. 21 disregarding the contribution of the second bolt row in tension. Each component was modelled with joint elements (JPH3) with different tension and compression behaviour (Fig. 20).

Fig. 22 illustrates the moment *versus* rotation curves obtained from the numerical simulations for several levels of axial force. The increase of resistance for low levels of compressive axial force observed in Fig. 23 is confirmed by the experimental results of Fig. 10.

Fig. 23 compares, test by test, the experimental and numerical results. It is clearly noticed that the application of the compressive axial force benefits the critical component of the tensile zone (end-plate in bending) and decreases the capacity of the critical component of the compression zone (beam flange in compression). The highest moment resistance is obtained for an axial force of 20% of the beam plastic resistance.

The corresponding M-N interaction diagram, plotted in Fig. 24 for the resistance of the joint, exhibits asymmetry around the pure bending situation ($N = 0$). This is a direct result of the different resistance between the tensile and compressive components.

6. Conclusions

Experimental results of the tests on flush end-plate beam-to-column joints loaded in bending and axial force that were carried out at the University of Coimbra were presented in this paper.

Based on the general principles of the component method, a numerical evaluation of the response of steel joints subjected to bending and axial forces was also presented in this paper. For the chosen flush end-plate joint, an increase of the moment resistance was noted for compressive axial force below 20% of the beam plastic resistance, clearly revealing the asymmetry of the response, while the same joint loaded in tension exhibited a reduction of the moment capacity.

These results highlight the need to review the current 10% limitation imposed by Eurocode 3 for joints subject to axial forces. Current experimental tests of extended end-plate joints subjected to bending moment and tension/compression axial force should provide additional clarification of these issues.

Acknowledgements

Financial support from “Ministério da Ciência e Tecnologia” - PRAXIS XXI research project PRAXIS/P/ECM/13153/1998 is acknowledged.

Financial support from “CAPES - Coordenação de Aperfeiçoamento de Pessoal de Nível Superior - Brazil” is gratefully acknowledged.

References

- Cerfontaine, F. (2000), “Etude analytique de l’interaction entre moment de flexion et effort normal dans les assemblages boulonnés” (in french), Travail de fin d’études du DEA en Sciences Appliquées, Département MSM, University of Liège, Belgium.
- Cruz, P., Silva, L.S., Rodrigues, D. and Simões, R. (1998), “Database for the semi-rigid behaviour of beam-to-column connections in seismic regions”, *J. Constructional Steel Research*, **46**(120), 1-3.
- EN 10002 (1990), “Metallic materials-tensile tests. Part1: method of test (at ambient temperature)”, *CEN, European Committee for Standardisation*.
- EN 10020 (1989), “Steel definition and classification”, *CEN, European Committee for Standardisation*.
- EN 10025 (1994), “Hot rolled products of non-alloy structural steels”, *CEN, European Committee for Standardisation*.
- Eurocode 3 (1998), ENV - 1993-1-1:1992/A2, Annex J, Design of Steel Structures - Joints in Building Frames. CEN, European Committee for Standardisation, Document CEN/TC 250/SC 3, Brussels.
- Eurocode 3 (2003), prEN 1993-1-8: 2003, Part 1.8: Design of Joints, Eurocode 3: Design of Steel Structures, Stage 49 draft., 5 May 2003. CEN, European Committee for Standardisation, Brussels.
- Faella, C., Piluso, V. and Rizzano, G. (2000), *Structural Steel Semi-Rigid Connections: Theory, Design and Software*, CRC Press LLC.
- FEA (2001), *LUSAS 13.3 User Manual*, FEA Ltd, UK.
- Jaspart, J.P., Braham, M. and Cerfontaine, F. (1999), “Strength of joints subjected to combined action of bending moment and axial force”, in *Proc. of the Conf. Eurosteel ’99*, CVUT Praha, Czech Republic, May 26-29, 465-468.
- Simões da Silva, L. and Coelho, A. G. (2000), “A analytical evaluation of the response of steel joints under bending and axial force”, *Comput. Struct.* **79**, 873-881.
- Simões da Silva, L., Lima, L., Vellasco, P. and Andrade, S. (2001), “Experimental and numerical assessment of beam-to-column joints under bending and axial force”, *Proc. of The First Int. Conf. on Steel & Composite Structures*, **1**, 715-722, June 2001, Pusan, Korea.

Notation

$M_{j,Rd}$: Connection flexural resistance
$S_{j,ini}$: Connection initial stiffness
N	: Axial force
E	: Young’s modulus
f_y	: Yielding stress
f_u	: Ultimate stress
k	: Elastic stiffness of each component
f_y^+	: Resistance of the component in tension
f_y^-	: Resistance of the component in compression
k_e^+	: Elastic stiffness of the component in tension
k_{pl}^+	: Plastic stiffness of the component in tension
k_e^-	: Elastic stiffness of the component in compression
k_{pl}^-	: Plastic stiffness of the component in compression
CC	